ACTA TEHNICA CORVINIENSIS – Bulletin of Engineering
Tome VII [2014] Fascicule 3 [July – September]
ISSN: 2067 – 3809

[1.] F. BOUMARAF, [2.] L. KHETTACHE,
[3.] R. ABDESSEMED, [4.] M.L. BENDAAS

POWERS AND TORQUE RIPPLE MINIMIZATION OF DOUBLY FED INDUCTION GENERATOR IN WECS USING SPACE VECTOR MODULATION

[1-4.] LEB - Research Laboratory, Department of Electrical Engineering, University of Batna, ALGERIA

Abstract: *Space Vector Pulse Width Modulation SVPWM Is the best modulation techniques to generate sinusoidal voltage and current due to its facility and efficiency with low harmonics distortion. In this paper we presents the study and power control of a variable speed wind energy conversion system based on a doubly Fed Induction Generator (DFIG) using space vector modulation to achieve control of active and reactive powers exchanged between the stator of the DFIG and the grid to ensure a Maximum Power Point Tracking (MPPT) of a wind energy conversion system and to reduce significantly Powers and Torque ripples. The Simulation results have shown good performances of the system under these proposed control Compared to PWM control strategies.*
Keywords: *Doubly fed induction generator, Space Vector PWM (SV-PWM), wind turbine, MPPT, WECS, pitch control*

INTRODUCTION

Nowadays wind energy has turned out to be one of the most important and promising sources of renewable energy after its progress during the last three decades. It has been the subject of much recent research and development; and he drawing the most attention from government, utilities and industry all over the world[2] due its smaller environmental impact and its renewable characteristic that contribute for a sustainable development [3].

The advances in wind turbine technology and the rapid development of power electronic devices and thus decreasing equipment costs, let a lot of researchers in wind power generation technologies to made necessary the design of powerful control systems in order to bring down the cost of electrical energy produced by the WECS to be competitive in the electricity market, and improved the dynamic behavior, resulting in the reduction of the mechanical Stress, fluctuation of the electrical power, the increase of the power capture[3]. The major part of the existing research works concerning variable speed wind turbines control is not only to capture the maximum power from the wind but, also, to improve the quality of power [4] and to converge the system for operating at unity power factor. The doubly fed induction generator (DFIG) which its stator winding is directly connected to the grid and its rotor winding is connected to the grid through a frequency converter introduces itself as one of the most important generators for wind energy conversion systems because of the following reasons: a higher energy yield, a reduction of mechanical loads, an extensive controllability of both active and reactive powers, less fluctuation in output power and a simpler pitch control.

However, the performance of a DFIG depends not only on the induction machine but also on the two PWM converters as well as how they are controlled. In order to comprehend DFIG power generation characteristics under different control conditions, this paper presents a detailed analysis of the comparative advantage of PWM and space vector pulse width modulation (SVPWM) control technique.

SVM CONTROL STRATEGY

Diagram of voltage space vectors

Space vector pulse width modulation (SVPWM) is a modulation technique that involves the generation of a reference vector V_{ref} representing a three phase sinusoidal voltage realized by switching between two nearest active vectors and

one zero vector switching sequence of a given power converter[6]. The desired output assigned V_{ref} will rotate in angular velocity equal to desired output converter frequency. The magnitude of this vector is related to the magnitude of the output voltage (SVM) and the time this vector takes to complete one revolution is egal as the fundamental time period of the output voltage [12]. Rotating to each active vector corresponds a switch sequence. There are eight possible output voltage vectors, or V_1, V_6 represented active switching ([011] [001] [101] [100] [110] [010]), and two zero voltage vectors, i.e. V_0 and V_7, corresponding to switching states ([000] and [111]) These two vectors allocate in the center of the circle. Figure 1 shows reference voltage vector V_{ref} and eight voltage vectors, which corresponds to the possible states of the inverter.

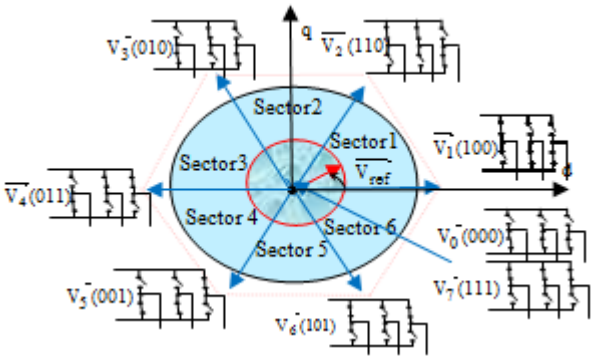

Figure1. Diagram of voltage space vectors

Implementation of the SVM Bloc

The vector V_{ref} is given by two components V_d ,v_q and angle(a). From Figure 2 the V_d, V_q, V_{ref}, and angle (a) can be determined as follows:

$$\begin{bmatrix} V_d \\ V_q \end{bmatrix} = \frac{2}{3}\begin{bmatrix} 1 & -\frac{1}{2} & -\frac{1}{2} \\ 0 & \frac{\sqrt{3}}{2} & -\frac{\sqrt{3}}{2} \end{bmatrix}\begin{bmatrix} V_{an} \\ V_{bn} \\ V_{cn} \end{bmatrix} \quad (1)$$

$$\left[\overline{V_{ref}}\right] = \sqrt{V_d^2 + V_q^2} \quad (2)$$

where:

$$a = tan\left(\frac{V_q}{V_d}\right) \quad (3)$$

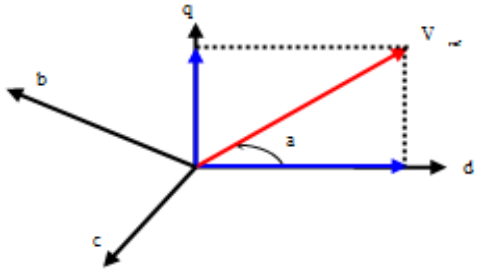

Figure 2. Voltage space vector and its components in (d, q).

An algorithm for Research angular sector is used to determine the sector (k= 1, 2, 3 ....6) as shown in Figure (3).

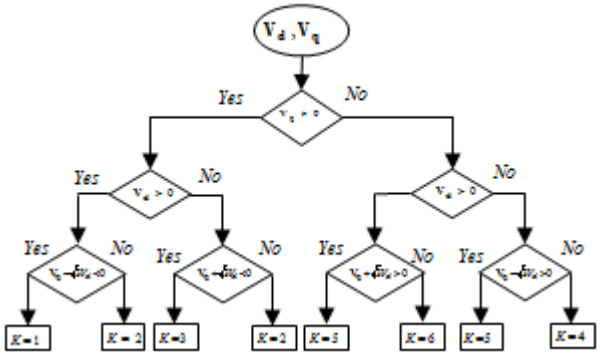

Figure 3. Algorithm for determining Sector K

In every sector, each voltage vector is synthesized by basic space voltage vector of the two side of sector and one zero vector. For example, in the first sector, V_{ref} is a synthesized voltage space vector and expressed by:

$$\int_0^{T_Z} \overline{V_{ref}} = \int_0^{T_1} \overline{V_1}dt + \int_{T_1}^{T_1+T_2} \overline{V_2}dt + \int_{T_1+T_2}^{T_1} \overline{V_0} \quad (4)$$

$$T_Z.\overline{V_{ref}} = (T_1.V_1 + T_1.V_2 + T_0.V_0) \quad (5)$$

$$T_Z = \frac{1}{f_Z} \text{ and } H = \frac{\overline{V_{ref}}}{2/3.V_{dc}} \quad (6)$$

where, T_0, T_1 and T_2 are the work times of basic space voltage vectors v_o, v_1 and v_2 respectively [8].

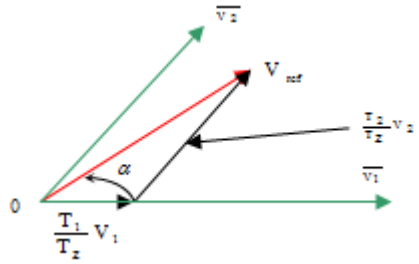

Figure 4. Reference vector as a combination of adjacent vectors at Sector 1.

The determination of the amount of times T_1 and T_2 is given by:

$$T_1 = \frac{\sqrt{3}T_Z\left|\overline{V_{ref}}\right|}{V_{dc}}\left(\sin\left(\frac{\pi}{3} - a + \frac{(n-1)}{3}\pi\right)\right) \quad (7)$$

$$T_1 = \frac{\sqrt{3}T_Z\left|\overline{V_{ref}}\right|}{V_{dc}}\left(\sin\left(\frac{n}{3}\pi\cos a - \cos\frac{n}{3}\pi\sin a\right)\right)$$

$$T_2 = \frac{\sqrt{3}T_Z\left|\overline{V_{ref}}\right|}{V_{dc}}\left(\sin\left(a - \frac{(n-1)}{3}\pi\right)\right) \quad (8)$$

$$T_2 = \frac{\sqrt{3}T_Z\left|\overline{V_{ref}}\right|}{V_{dc}}\left(\sin a\sin\frac{(n-1)}{3}\pi - \cos a\sin\frac{(n-1)}{3}\pi\right)$$

$$T_0 = (T_Z - T_2 - T_2) \quad (9)$$

where, the sector (n) = 1 through 6.
The switching time at each sector is summarized in the following Table [8].

Table 1. The switching time

sector	Switches(s_1, s_3, s_5)	Switches(s_4, s_6, s_2)
1	$s_1=T_1+T_2+T_0/2$ $s_3=T_2+T_0/2$ $s_5=T_0/2$	$s_4=T_0/2$ $s_6=T_1+T_0/2$ $s_2=T_1+T_2+T_0/2$
2	$s_1=T_1+T_0/2$ $s_3=T_1+T_2+T_0/2$ $s5=T_0/2$	$s_4=T_2+T_0/2$ $s_6=T_0/2$ $s_2= T_1+T_2+T_0/2$
3	$s_1=T_0/2$ $s_3= T_1+ T_2+ T_0/2$ $s_5= T_2+ T_0/2$	$s_4= T_1+ T_2+T0/2$ $s_6= T_0/2$ $s2= T_1+ T_0/2$
4	$s_1= T_0/2$ $s_3= T_1+ T_0/2$ $s_5= T_1+ T_2+ T_0/2$	$s_4= T_1+T2+T0/2$ $s_6= T_2+ T_0/2$ $s_2= T_0/2$
5	$s_1= T_2+ T_0/2$ $s_3= T_0/2$ $s_5= T_1+ T_2+ T_0/2$	$s_4= T_1+ T_0/2$ $s_6= T_1+ T_2+ T_0/2$ $s_2= T_0/2$
6	$s_1= T_1+ T_2+ T_0/2$ $s_3= T_0/2$ $s_5= T_1+ T_0/2$	$s_4= T_0/2$ $s_6= T_1+ T_2+T0/2$ $s_2= T_2+ T_0/2$

WECS Modeling

The general turbine model with doubly fed induction generator is shown in Figure 5.

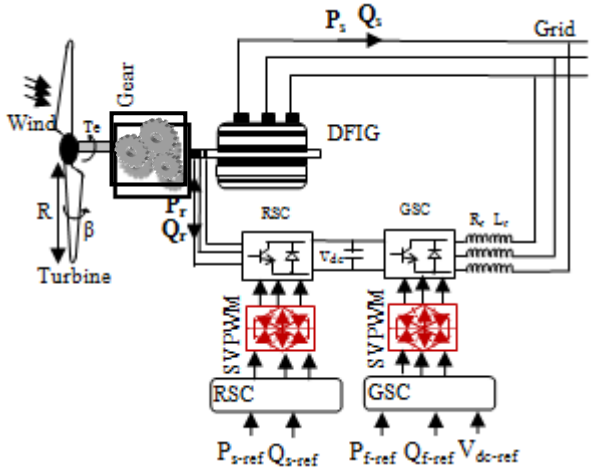

Figure 5. Wind turbine system with DFIG

Wind Turbine Model

The wind turbine is modeled in terms of optimal tracking, to provide maximum energy capture from the wind. The aerodynamic model of the wind turbine gives a coupling between the wind speed and the mechanical torque produced by the wind turbine. The mechanical power Pt produced by the wind turbine rotor can be defined as [11]:

$$p_t = \frac{1}{2} c_p(\lambda, \beta).\rho. \quad s.v^3 \qquad (10)$$

with :

$$\lambda = \frac{\Omega_t}{v}.R \qquad (11)$$

where P_t (w) the aerodynamic power; P_v (w) wind power available in the rotor swept area; ρ (kg/m³) the air density; S (m²) the rotor disk area, R (m) the rotor radius; ν (m/s) the wind speed; and Cp the power coefficient which is a function of the tip speed ratio λ (ratio between blade tip speed and wind speed) and β the pitch angle of rotor blades.

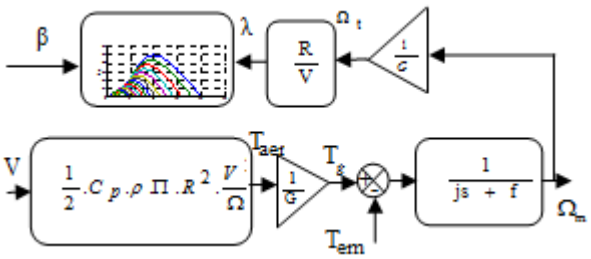

Figure 6. Wind turbine model

The power coefficient is defined by:

$$C_p(\lambda,\beta) = C_1\left(\frac{C_2}{\lambda_i} - C_3.\beta - C_4\right)e^{\frac{-C_5}{\lambda_i}} + C_6\lambda \qquad (12)$$

where

$$\frac{1}{\lambda_i} = \frac{1}{\lambda + 0.08.\beta} - \frac{0.035}{1+\beta^3} \qquad (13)$$

with: $c_1 = 0.5176$, $c_2 = 116$, $c_3 = 0.4$, $c_4 = 5$, $c_5 = 21$, $c_6 = 0.0068$

On Figure 8 is represented this coefficient in function of λ and for different values of pitch angle β of the blades. This curve is characterized by the optimal point (λopt=9, Cp-max=0.5, β=2°) corresponding to the maximum power coefficient Cp and therefore the maximum mechanical power recovered

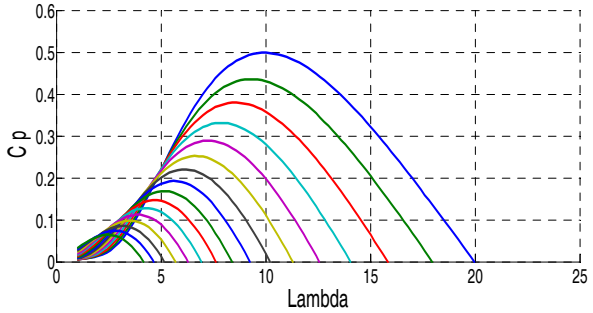

Figure 7. Characteristic $C_p = f(\lambda_{opt})$

$$\Omega_t = \frac{\lambda_{opt}}{R}.v \qquad (14)$$

The torque at the shaft neglecting losses in the drive-train is given by:

$$T_t = \frac{P_t}{\Omega_t} = \frac{R.P_t}{\lambda.v} = \frac{C_p \rho \pi^2 R_t^3 v^2}{2\lambda} \qquad (15)$$

and $$C_t = \frac{C_p}{\lambda} \quad (16)$$

For our model we'll assume the stiffness and damping are neglected, and then the dynamic equations of the drive-train can be obtained with a model to a mass in this case described by:

$$T_g - T_{em} = J \frac{d\Omega_m}{dt} \quad (17)$$

The equivalent moment of inertia is:

$$J = J_g + \frac{J_t}{G^2} \quad (18)$$

the gear ratio between the turbine and the generator:

$$G = \frac{\Omega_t}{\Omega_g} \quad (19)$$

Doubly-Fed Induction Generator

The DFIG voltage and flux equations, expressed in the Park reference frame, are given by.

$$\begin{aligned} V_{sd} &= R_s I_{sd} + \frac{d}{dt}\varphi_{sd} - \omega_s \varphi_{sq} \\ V_{sq} &= R_s I_{sq} + \frac{d}{dt}\varphi_{sq} + \omega_s \varphi_{sd} \end{aligned} \quad (20)$$

$$\begin{aligned} \varphi_{sd} &= L_s I_{sd} + M I_{rd} \\ \varphi_{sq} &= L_s I_{sq} + M I_{rq} \\ \varphi_{rd} &= L_r I_{rd} + M I_{sd} \\ \varphi_{rq} &= L_r I_{rq} + M I_{sq} \end{aligned} \quad (21)$$

Moreover, the electromagnetic torque is given by:

$$C_e = p\frac{M}{L_s}\left(I_{rq}\varphi_{sd} - I_{rd}\varphi_{sq}\right) \quad (22)$$

The stator resistance of the DFIG is neglected and the stator flux φ_s is set aligned with the d axis and assumed to be constant (it is the case of a powerful and stable grid) [12]. Then, we can write $\varphi_{sd} = \varphi_s, \varphi_{sq} = 0$

Consequently, the stator voltages and fluxes can be rewritten as follows:

$$\begin{aligned} V_{sd} &= \frac{d}{dt}\varphi_s = 0 \\ V_{sq} &= \omega_s \varphi_s \end{aligned} \quad (23)$$

$$\begin{aligned} \varphi_{sd} &= L_s I_{sd} + M I_{rd} \\ 0 &= L_s I_{sq} + M I_{rq} \end{aligned} \quad (24)$$

Hence, the torque equation can be written as follow

$$T_{em} = p\frac{M}{L_s} I_{rq}\varphi_{sd} \quad (25)$$

The stator active and reactive power and voltages are given by:

$$\begin{aligned} P &= V_{sd} I_{sd} + V_{sq} I_{sq} \\ Q &= V_{sq} I_{sd} - V_{sd} I_{sq} \end{aligned} \quad (26)$$

From equation (16), we obtain:

$$\begin{aligned} P &= -V_s \frac{M}{L_s} I_{rq} \\ Q &= -V_s \frac{M}{L_s} I_{rd} + V_s \frac{\varphi_s}{L_s} \end{aligned} \quad (27)$$

From the last equation, we can see that the electromagnetic torque and the active power will only depend on the q-axis rotor current, while the reactive power may be controlled through the rotor current I_{rd}.

the rotor voltage equations can be defined as:

$$\begin{aligned} V_{rd} &= R_r I_{rd} + (L_r - \frac{M^2}{L_s})\frac{dI_{rd}}{dt} - g\omega_s(L_r - \frac{M^2}{L_s})I_{rq} \\ V_{rq} &= R_r I_{rq} + (L_r - \frac{M^2}{L_s})\frac{dI_{rq}}{dt} + g\omega_s(L_r - \frac{M^2}{L_s})I_{rd} + g\frac{MV_s}{L_s} \end{aligned} \quad (28)$$

Rotor Side Converter

This converter controls the active and reactive powers generated by the stator of the DFIG and delivered to the grid by controlling the rotor currents of the DFIG (Figure 8). The real active and reactive powers are compared to their references, and then two PI controllers are used. The outputs of these controllers represent the direct and quadrature components of the current references [14]

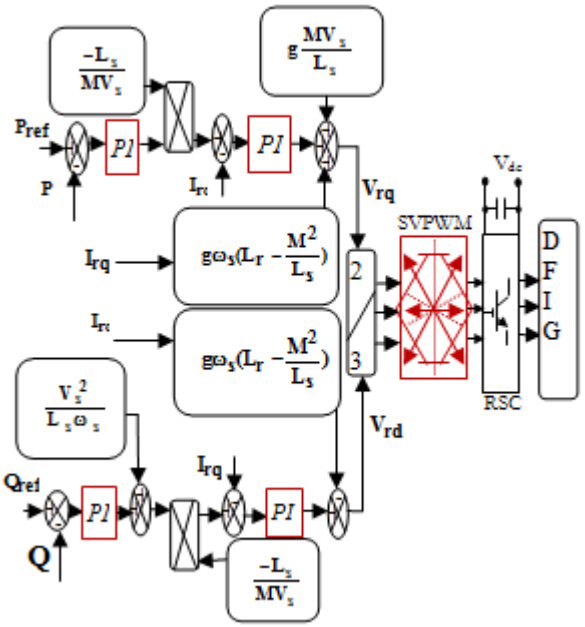

Figure 8. Control of the RSC

Grid Side Converter

The objective of the grid side converter is to regulate the DC-link voltage and to set a unit

power factor. The topology of grid-side converter is shown in Figure 9.

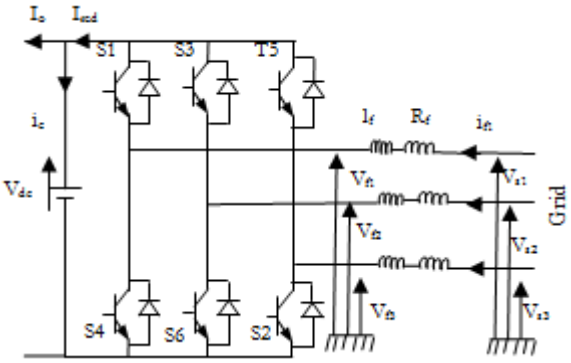

Figure 9. Grid side converter

Based on the circuit topology, the mathematical model of inverter in three-phase static abc coordinates can be drawn as follows:

$$\begin{aligned} V_{f1} &= -R_f i_{f1} - l_f \frac{di_{f1}}{dt} + v_{s1} \\ V_{f2} &= -R_f i_{f2} - l_f \frac{di_{f2}}{dt} + v_{s2} \\ V_{f3} &= -R_f i_{f3} - l_f \frac{di_{f3}}{dt} + v_{s3} \end{aligned} \quad (29)$$

In the d, q reference frame:

$$\begin{aligned} V_{fd} &= -R_f i_{fd} - l_f \frac{di_{fd}}{dt} + \omega_s l_f i_{fq} + v_{sd} \\ V_{fq} &= -R_f i_{fq} - l_f \frac{di_{fq}}{dt} + \omega_s l_f i_{fd} + v_{sq} \end{aligned} \quad (30)$$

The active and reactive powers (P_f and Q_f) can be both expressed by using Park components of supply voltage(v_{fd} and v_{fq}) and line current(i_{fd} and i_{fq}) as follows:

$$\begin{aligned} P_f &= v_{fd} i_{fd} + v_q i_{fq} \\ Q_f &= v_{fq} i_{fd} - v_d i_{fq} \end{aligned} \quad (31)$$

we can find the reference currents ($i_{fd\text{-}ref}$, $i_{fq\text{-}ref}$), which allows setting the desired reference active and reactive powers ($P_{f\text{-}ref}$, $Q_{f\text{-}ref}$), as follows:

$$\begin{aligned} i_{fd\text{-}ref} &= \frac{Q_{f\text{-}ref}}{v_{sq}} \\ i_{fq\text{-}ref} &= \frac{P_{f\text{-}ref}}{v_{sq}} \end{aligned} \quad (32)$$

The unity power factor is obtained simply by setting the reactive power reference null. The DC reference voltage $V_{dc\text{-}ref}$ is compared to the measured DC voltage across the capacitor V_{dc}. The DC voltage corrector regulates the DC bus and sets the active power $P_{c\text{-}ref}$ which is necessary to charge the capacitor to the desired value. The reference active power Pf- ref is obtained after being calculated the Pc-ref. The evolution of the DC voltage V_{dc} is given by the following equation:

$$\begin{aligned} C.\frac{dv_{dc}}{dt} &= (i_{red} - i_o) \\ i_c &= i_{red} - i_o \end{aligned} \quad (33)$$

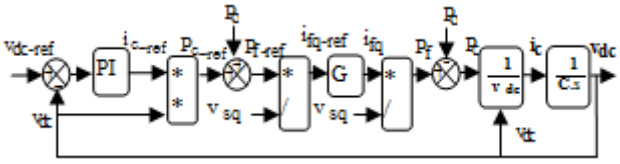

Figure 10. Bloc Diagram of the DC Bus Control

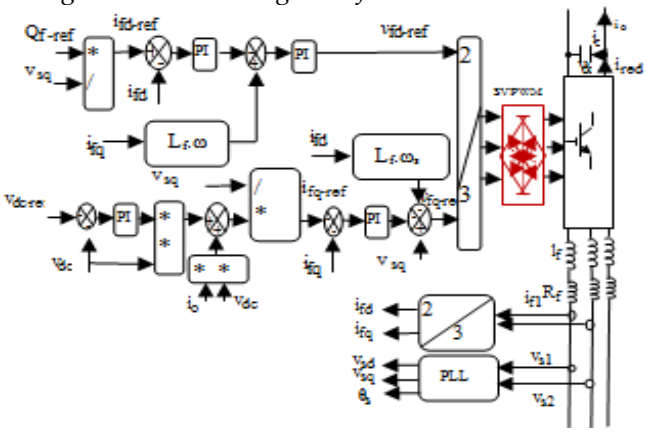

Figure 11. Grid side converter control

SIMULATION RESULTS

In order to made a comparison between the proposed control strategies PWM (SV-PWM) for a doubly fed induction generator (DFIG)-based wind energy conversion system shown in Figure (5), all the matlab simulations are carried out in the same operation conditions.

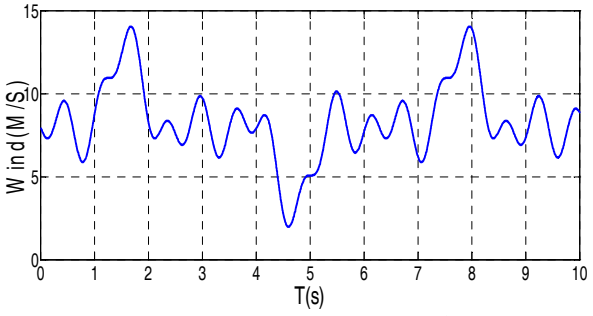

Figure 12. Wind speed profile

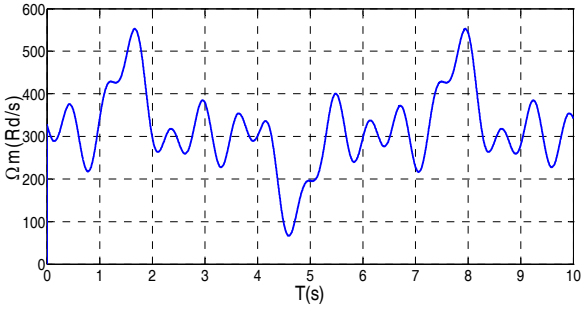

Figure 13. Mechanical speed

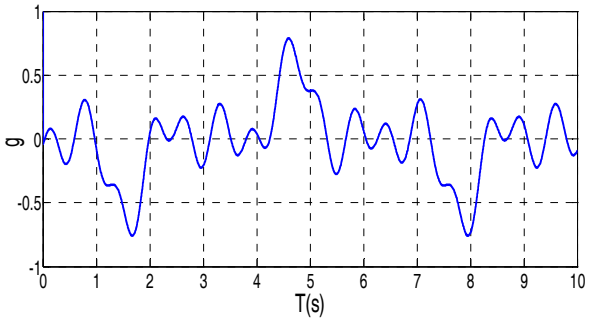

Figure 14. Slip variation of the grid-connected DFIG

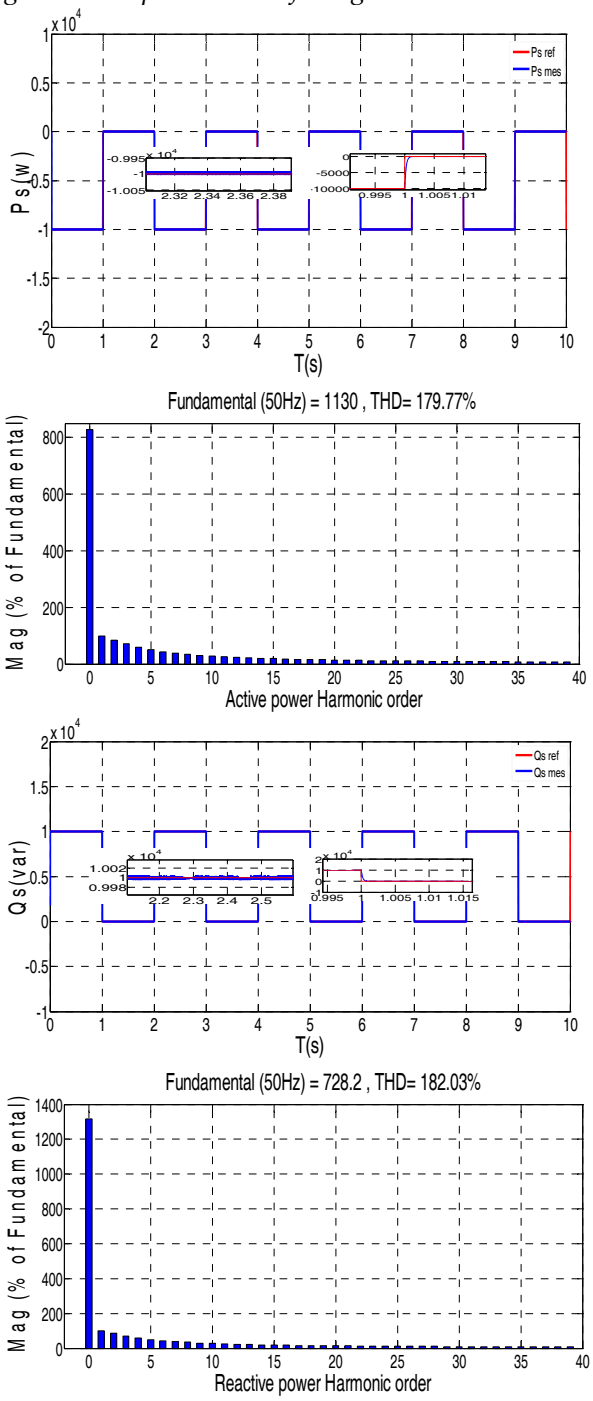

Figure 15. (a) Stator active and reactive powers with SVM

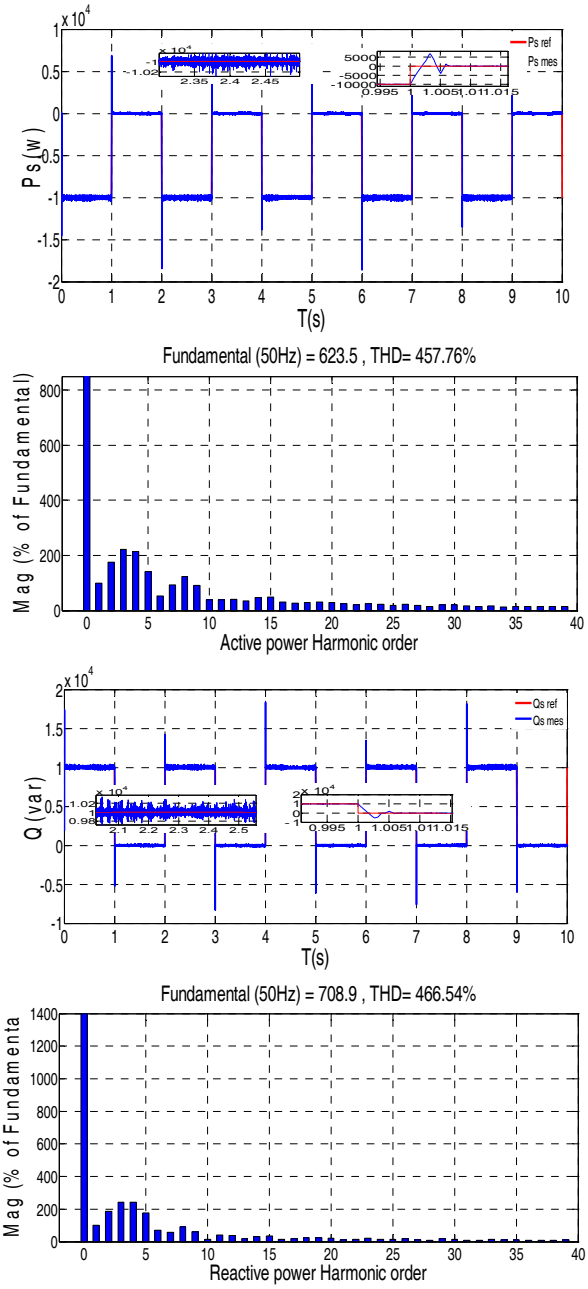

Figure 15. (b) Stator active and reactive powers with PWM

Variable speed operation in the DFIG tracking curve effects higher power output from the wind. The direction of the power flow through the converters depends on the operating point of the generator.

In the sub-synchronous operation mode, the stator of DFIG supplies power to the grid and also the slip power to the rotor via the slip rings and the power converter. In the super-synchronous operation mode, both the stator output power and the rotor slip power are fed into the grid. In all simulation results presented, by comparing the current, torque, active and reactive power THD

between the proposed control strategies it can be observed a much better behavior of the SV-PWM performance as compared to PWM, achieving the objectives of the present work, which was to reduce the torque and power ripple and consequently improve the power exchanged between the stator of the DFIG and the power network.

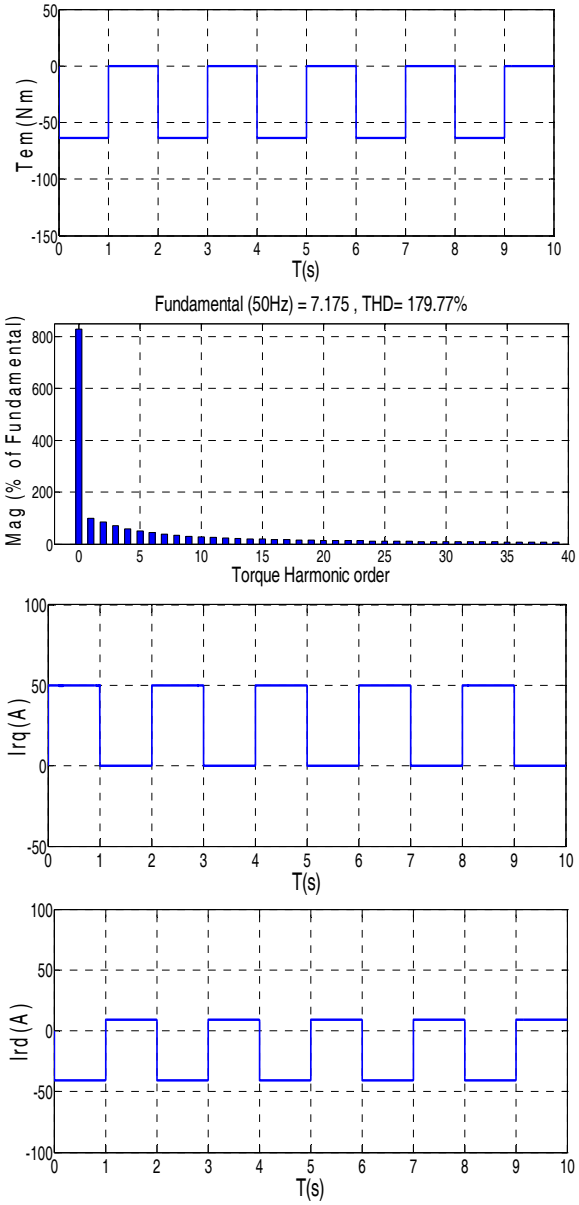

Figure 16(a). Torque and rotor currents with SVM

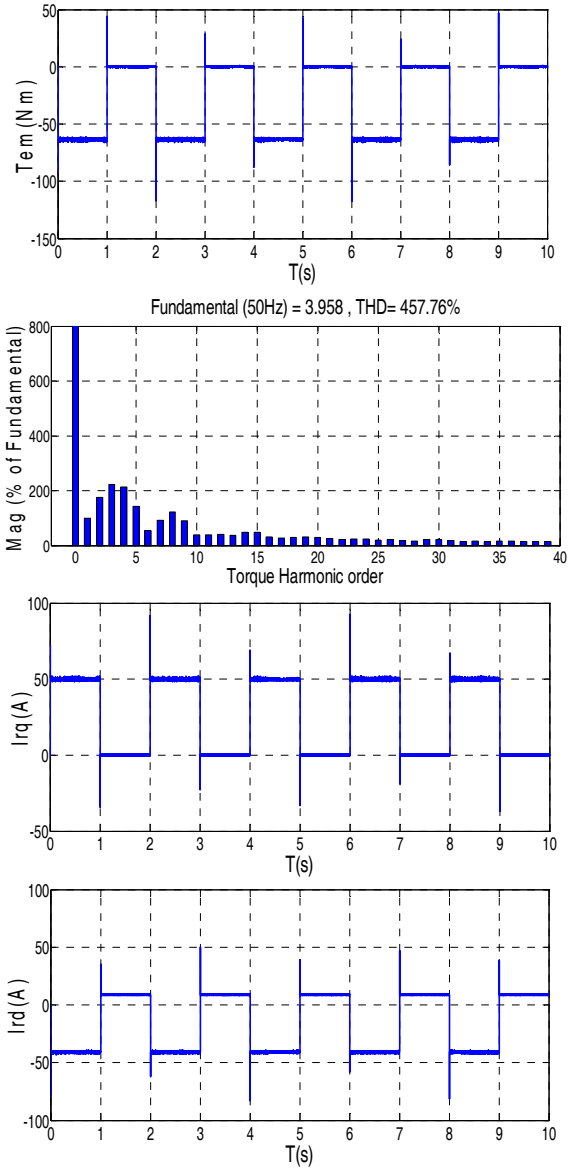

Figure 16(b). Torque and rotor currents with PWM

Simulation results show good decoupling between stator active and reactive power and proven that both control strategies are able to offer convergence of the dynamic response of the system to the reference values despite wind variations. The proposed scheme ensures perfect tracking of maximum captured power and improves good dynamics and provides less harmonics in rotor currents.

CONCLUSION

The paper has presented a model for a wind turbine generation system based on a doubly fed induction generator with a stator directly connected to the grid and a rotor connected to the grid through SVPWM converte.

A detailed modeling of the mechanical dynamics, the wind turbine electrical system, and the converter been presented.

The obtained results demonstrate that the proposed DFIG system control operating at the variable speed may be considered as an interesting way for problems solution in renewable energy area.

References

[1.] W. Yu, J. Lai and S.Y. Park, «An Improved Zero-Voltage Switching Inverter Using Two Coupled Magnetic in One Resonant Pole» IEEE Trans. on

Power Electron., Vol.25, No.4, pp.952-961, April.2010.

[2.] *J. Hua, Y. Hea and L Xub, «Improved rotor current control of wind turbine driven doubly-fed induction generators during network voltage unbalance»,Electric Power Systems Research 80 (2010) 847–856*

[3.] *A. K. Mishra, L. Ramesh, S.P. Chowdhury, S.Chowdhury, «Review of Wind Turbine System and its Impact for Grid Stability», Journal of Electrical Engineering. Vol.11, Issue 1. 2011. pp. 153–165.*

[4.] *L. Shuhui, T.A. Haskew, «Analysis of Decoupled d-q Vector Control in DFIG Back-to-Back PWM Converter», IEEE CNF Power Engineering. June 2007. pp.1-7.*

[5.] *Y. Bekakra, D. B. attous, «Active and Reactive Power Control of a DFIG with MPPT for Variable Speed Wind Energy Conversion using Sliding Mode Control», World Academy of Science, Engineering and Technology 60 2011.*

[6.] *H.Karimi-Davijani, A.Sheikholeslami, R. Ahmadi, and H. Livani, «Active and reactive power control of DFIG using SVPWM converter», in Proc.of IEEE UPEC, pp.1-5, 2008.*

[7.] *Badrul H. Chowdhury, and Srinivas Chellapilla, «Double-fed induction generator control for variable speed wind power generation», Electric Power Systems Research, Volume 76, Issues 9-10, June 2006, pp.786-800.*

[8.] *J.W Jung, A. Keyhani, «Space Vector PWM Inverter», Departement of Electrical and Computer the Ohio State University, 2005.*

[9.] *R. Penaa, R. Cardenasb, E. Escobarb, J. Clarec, P. Wheelerc, « Control strategy for a doubly-fed induction generator feeding an unbalanced grid or stand-alone load, Electric Power Systems Research, Vol. 79, pp. 355- 364, 2009.*

[10.] *A. M. Eltamaly, A. I. Alolah, M. H. Abdel-Rahman, « Modified DFIG control strategy for wind energy applications», SPEEDAM 2010, International Symposium on Power Electronics, Electrical Drives, Automation and Motion, 2010 IEEE, pp. 659-653, 2010.*

[11.] *M. Machmoum, F. Poitiers, «Sliding mode control of a variable speed wind energy conversion system with DFIG», International Conference and Exhibition on Ecologic Vehicles and Renewable Energies, MONACO, March 26-29 (2009).*

[12.] *M. Saeedifard, H. Nikkhajoei, R. Iravani and A. Bakhshai, «A Space Vector Modulation Approach For A Multi- Module HVDC Converter System», IEEE Transactions on Power Delivery, Vol.22, No.3, PP.1643-1654, July, 2007.*

[13.] *Choon Yik Tang, Yi Guo, John N. Jiang, «Nonlinear Dual-Mode Control of Variable-Speed Wind Turbines with Doubly Fed Induction generators»,IEEE,Transactions on Control Systems Technology, July 2011, 19 (4), pp. 744-756*

[14.] *Yao Xing-jia, Liu Zhong-liang, Cui Guo-sheng, «Decoupling control of Doubly-Fed Induction Generator based on Fuzzy-PI Controller», IEEE Trans. Mechanical and Electrical Technology (ICMET 2010) , pp 226-230 ,2010.*

[15.] *Md. Rabiul Islam1, Youguang Guo, Jian Guo Zhu, «Steady State Characteristic Simulation of DFIG for Wind Power System», IEEE Trans. Electrical and Computer Engineering (ICECE), pp. 151-154, 2011.*

[16.] *T. Luu, A. Nasiri, «Power Smoothing of Doubly Fed Induction Generator for Wind Turbine Using Ultra capacitors», IEEE Trans. IECON 2010 - 36th Annual Conference., pp. 3293-3298, 2010.*

[17.] *C.O. Omeje, D.B. Nnadi, and C.I. Odeh, «Comparative Analysis of Space Vector Pulse-Width Modulation and Third Harmonic Injected Modulation on Industrial Drives», The Pacific Journal of Science and Technology, Volume 13. Number 1. May 2012 (Spring).*

[18.] *H. Zhang, Q. Wang, E. Chu, Xi. Liu, and L. Hou, «Analysis and Implementation of A Passive Lossless Soft-Switching Snubber for PWM Inverters», IEEE Trans. on Power Electron. Vol. 26, No.2, pp. 411- 426, Feb.201.1*

[19.] *R. Huang and S. K. Mazumder, «A Soft Switching Scheme for Multiphase DC/Pulsating-DC Converter for Three-Phase High-Frequency-Link Pulse width Modulation (PWM) Inverter», IEEE Trans. on Power Electron.,Vol.25,No.7,pp.1761-1774,July.2010. Renewable Energy, Vol. 35, pp. 1033-1042, 2010*

ACTA Technica CORVINIENSIS
BULLETIN OF ENGINEERING
ISSN:2067-3809